Supplementary Information

Operating Principles of Interconnected Feedback Loops Driving Cell Fate Transitions

Mubasher Rashid[1,*] and Abhiram Hegade [2]

[1]Department of Mathematics and Statistics, Indian Institute of Technology Kanpur, Kanpur - 208016, India.
[2]Department of Mathematics, University of Florida, Gainesville - 32601, FL, USA.

Email id: mubasher@iitk.ac.in, mubasherrashid@gmail.com

Supplementary Note 1

S1. Topology-dependent steady-state distribution in larger serial and hub networks

In this section, we constructed larger size (10 nodes) serial and hub HDFLs and analyzed the probability distribution (in percentage) of mono, bi, tri, and tetrastable states. We show that our findings for small serial and hub HDFLs with three, four, and five nodes also hold for larger HDFLs. As shown in Fig. 1A, the serial network exhibits equal (~20%) possibilities for bi, tri, and tetrastable states and quite a lesser chance (~10%) for monostability, implying that serial topology favors higher-order stability. In Fig. 1B, however, we see that the hub topology leads to bistability (~85%) with little chance for monostability (~15%). This indicates that larger hub networks are strictly bistable systems.

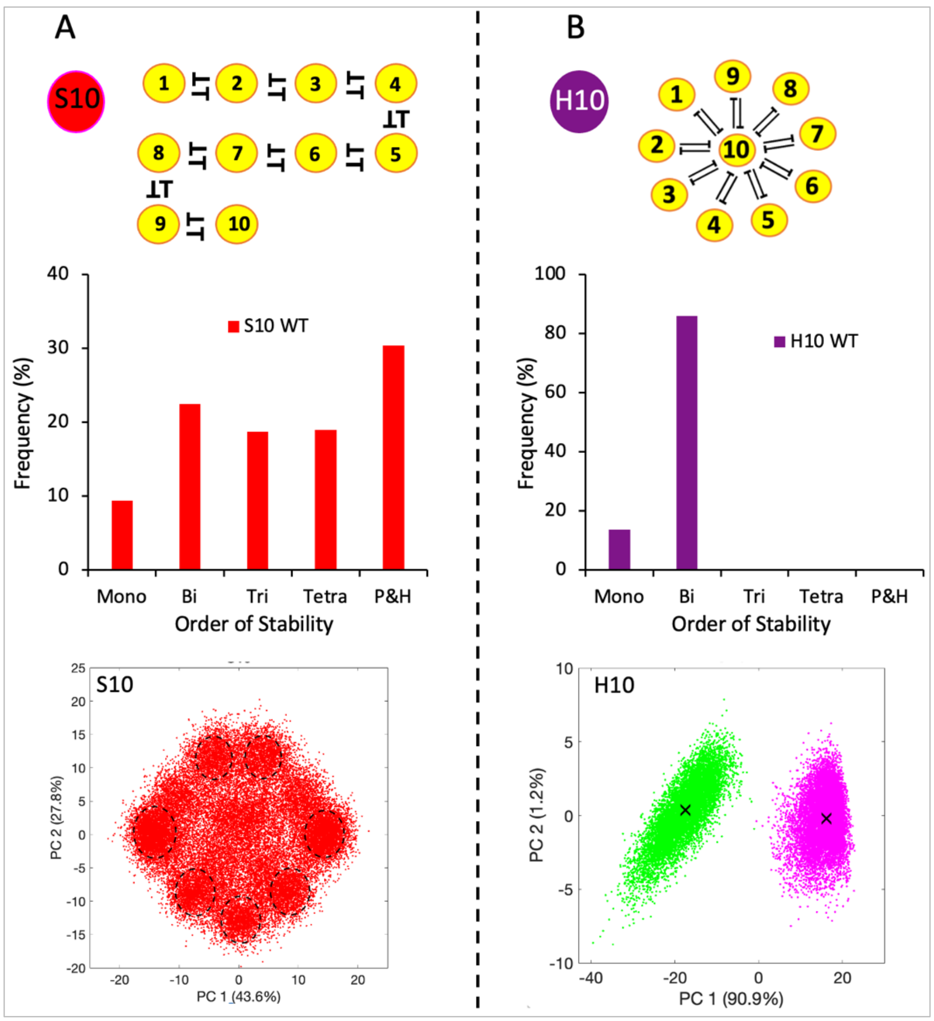

Supplementary Fig 1. Schematics and SSD of larger serial and hub type HDFLs, each having ten nodes and nine toggle switches. (A) The ST topology exhibits almost equal (~20%) possibility for bi, tri, and tetrastable states with the occurrence of some (<10%) monostable states as well. (B) The hub topology shows complete dominance of bistability (~85%) over monostability (~15%) while also eliminating the chance for tri-and tetrastable states. P&H denotes penta- and higher-order states that collectively include five and up to ten states. The lower horizontal panel shows in silico gene expression projected on the 1st and 2nd principal component axes and clustering of multiple states in S10 and just two states in H10.

S2. Autoregulations enable higher-order stability.

In this section, we investigate the effect of autoregulations on network dynamics. After self-activating a particular node in a network, we simulate its emergent dynamics and compare the steady-state distribution with the corresponding WT (no self-activated nodes) network. We repeat this process until all the nodes in the network are self-activated. In the plots below, the first bars (dark color) corresponding to each order of stability, i.e., mono, bi, tri, tetra, and P&H stability, compose the SSD of the WT network. The bars at the second place compose the SSD of the network with a single node self-activated, the bars at the third place compose the SSD of the network with two nodes self-activated, and so on. As shown, as more nodes get self-activated, the frequency of mono-and bistable states decrease which is compensated by increase in the frequency of tri-and tetrastable states. The peak of SSD thus shifts from lower-order to higher-order stability. Interestingly, this trend becomes more evident as network size increases and can be noticed throughout the networks. We thus conclude that regardless of the topology, networks with self-activations tend to exhibit multiple alternative states.

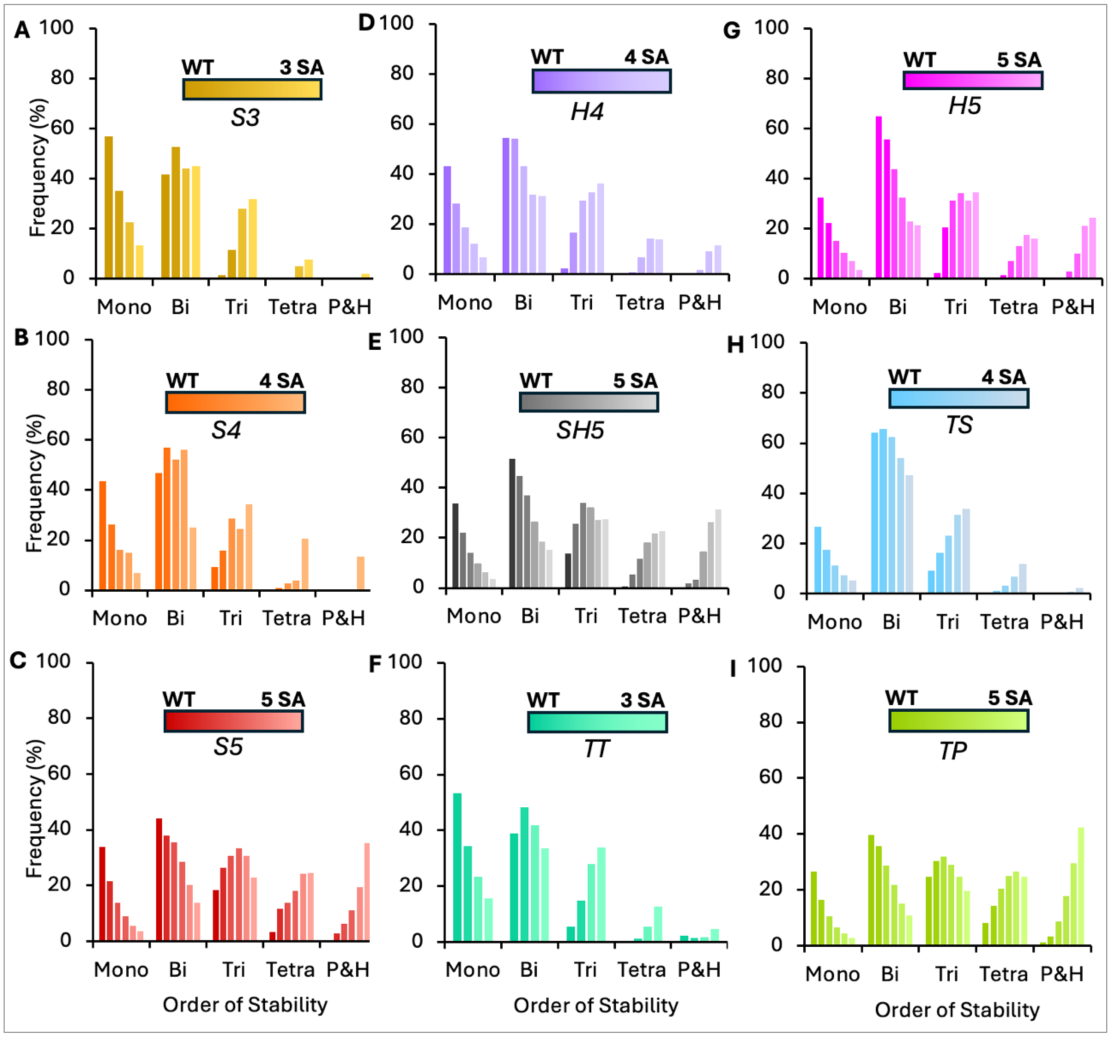

Supplementary Fig 2. Bar plots showing the steady-state distribution (SSD) of all the WT networks and their self-activated counterparts. The first vertical panel contains HDFLs having serial topology, S3, S4, S5. As we move along the first horizontal panel, network becomes more hub. At the center, SH5 is a mixed serial/hub network. Also, TT, TS, TP are cyclic HDFLs with three, four, and five nodes. The left-extreme of the color gradient panel in each network represents WT (unperturbed) network. As the color gets darker, the number of self-activations in the network increases. The right-extreme of the color gradient panel represents the network with all nodes self-activated.

S3. Topologically distinct networks with the same number of nodes can exhibit different dynamics

The data reveals that topologically distinct networks with the same node count can exhibit different numbers of alternative states. It also shows that each cyclic network allows an extra cluster than the serial network with the same number of nodes. For instance, TT allows three while S3 allows two states (top horizontal panel), TS possibly allows four while S4 allows three states (middle horizontal panel), and TP exhibits five while S5 exhibits four states (lower horizontal panel). This shows that cyclic networks operate closer to serial networks and both of these operate opposite to hub networks (H4, H5) which show only a few states (just two).

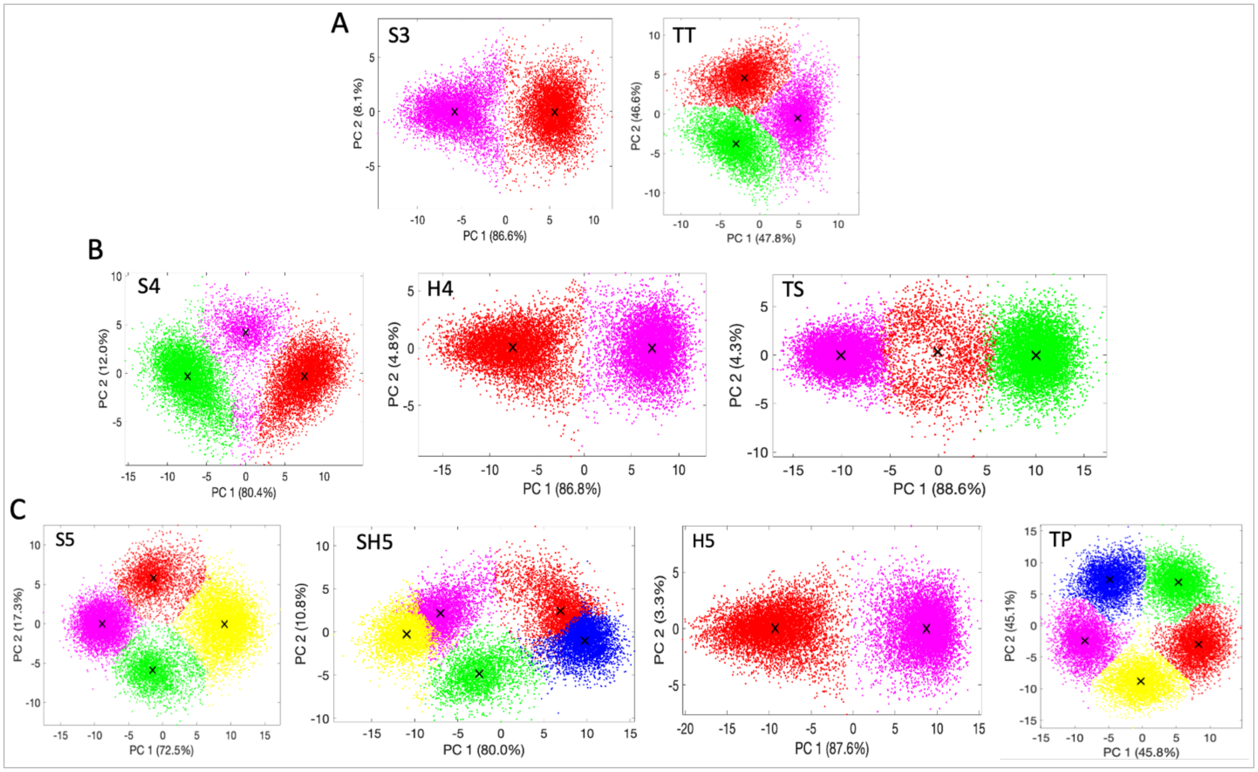

Supplementary Fig 3. Comparative analysis of alternative states (clusters) in topologically distinct networks with the same number of nodes. (A) Three-node networks show two (in S3) and three (in TT) states. (B) Four-node networks show three (in S4), two (in H4), and three to four (in TS) states. (C) Five-node networks four (in S5), five (in SH5), two (in H5), and five (in TP) states.

S4. Perturbations to restrict the dimension of state space of the networks.

Here we analyze the effect of single-edge perturbations (ED and ESR) on the SSD of HDFLs. We take an HDFL and randomly delete an edge or change the sign of an edge from repression to activation. We simulate the two perturbed networks and compare their SSD with the WT counterpart. A similar procedure is carried out throughout all HDFLs. For all networks, the data emphasize that both edge perturbations significantly increase lower-order stability which is compensated by a decrease in higher-order stability. The SSD peak therefore shifts to the left. We also observe that an ESR is more effective than an ED in increasing lower-order stability since each ESR results in more frequency of lower-order stability than an ED. Furthermore, the data depicts that when all the network nodes are self-activated single ED and single ESR become ineffective in reducing (increasing) the frequencies of higher-order (lower-order) states.

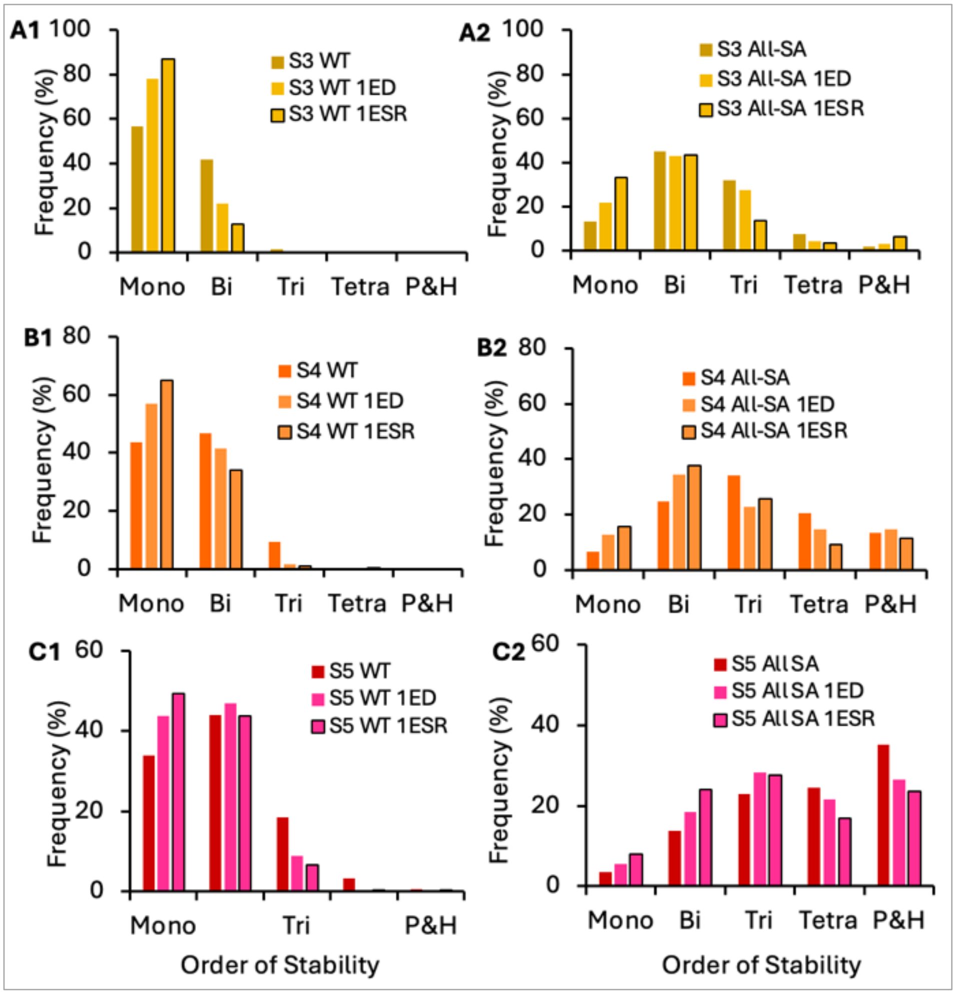

Supplementary Fig 4. Effect of single Edge Deletion (ED) and single Edge Sign Reversal (ESR) on the SSD of Serial HDFLs. (A1-C1) Bar graphs showing a comparison of SSDs of WT Serial HDFLs with their two perturbed networks. (A2-C2) Same as the left panel, except that all the network nodes are self-activated.

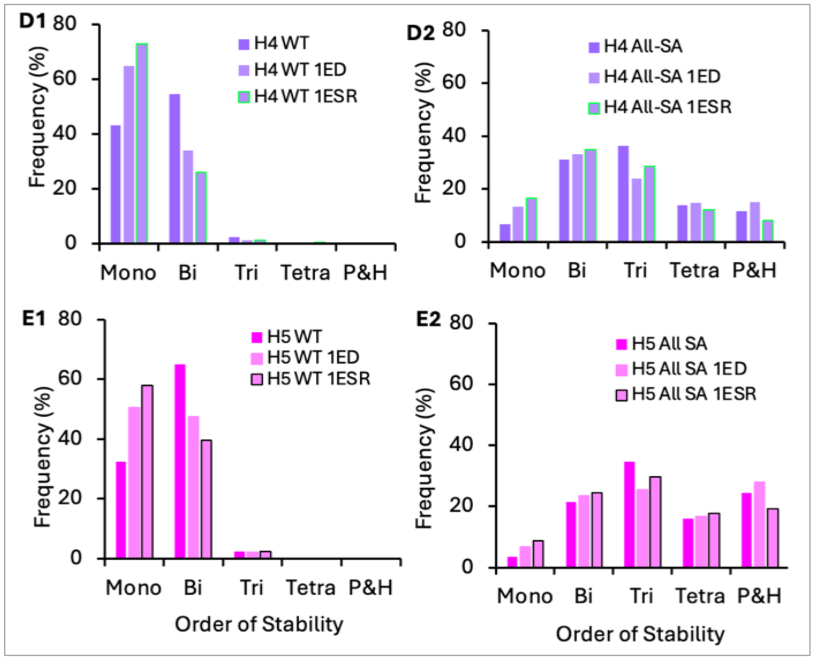

Supplementary Fig 5. Effect of single Edge Deletion (ED) and single Edge Sign Reversal (ESR) on the SSD of Hub HDFLs. (A1-C1) Bar graphs showing comparison of SSDs of WT Hub HDFLs with their two perturbed networks. (A2-C2) Same as left panel, except that all the network nodes are self-activated.

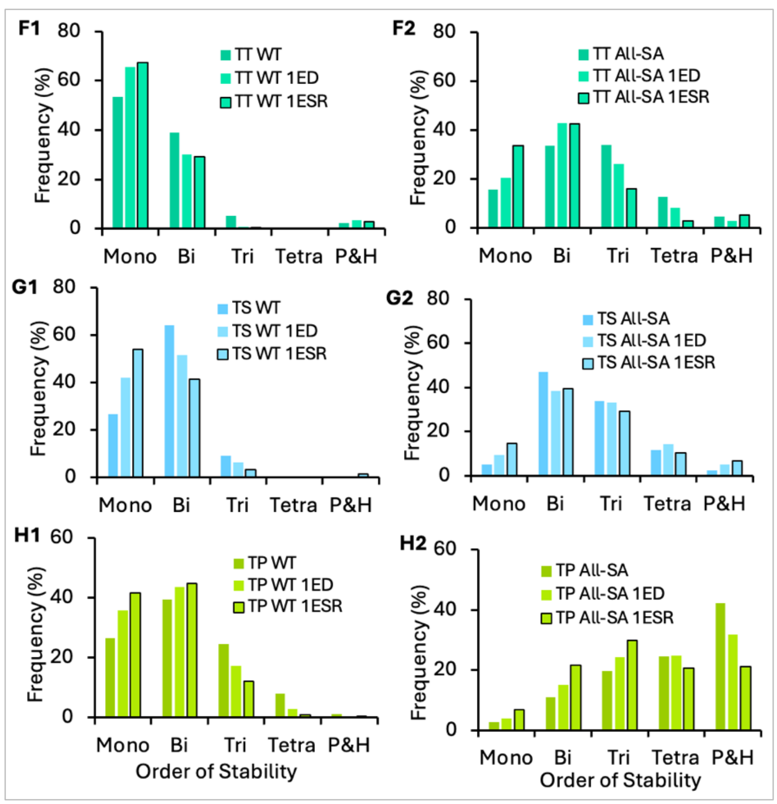

Supplementary Fig 6. Effect of single Edge Deletion (ED) and single Edge Sign Reversal (ESR) on the SSD of Cyclic HDFLs. (A1-C1) Bar graphs showing comparison of SSDs of WT Cyclic HDFLs with their two perturbed networks. (A2-C2) Same as left panel, except that all the network nodes are self-activated.

S5. Effect of increasing the number of edge perturbations.

Here we identify the number of perturbations that are required to convert a multistable HDFL into a monostable HDFL. In general, we see that we need to break all PFLs (equivalent to the number to toggle switches) in the network to achieve monostablity. Since serial-and hub type networks having n nodes contain $(n-1)$ PFLs. In other words, in an n node serial or hub type network, $(n-1)$ PFLs need to be eliminated to achieve a unique steady state. Further, any cyclic network has as many nodes as toggle switches and we observe that even after deleting all PFLS these networks still don't become completely monostable, though the frequency of monostable states is the highest after breaking all the loops. This may be attributed to a unique property of cyclic networks as even after breaking all loops, there still remains the possibility of the existence of a "global" feedback (involving all nodes) or a feedforward loop in these networks. On the other hand, we see that in networks with all the self-activated nodes, only mono or bistable states are never possible. In fact, with maximum perturbations, HDFLs show almost equal possibilities for mono, bi, and tristable states. This again reiterates that networks with autoregulated nodes always tend to exhibit higher-order stability.

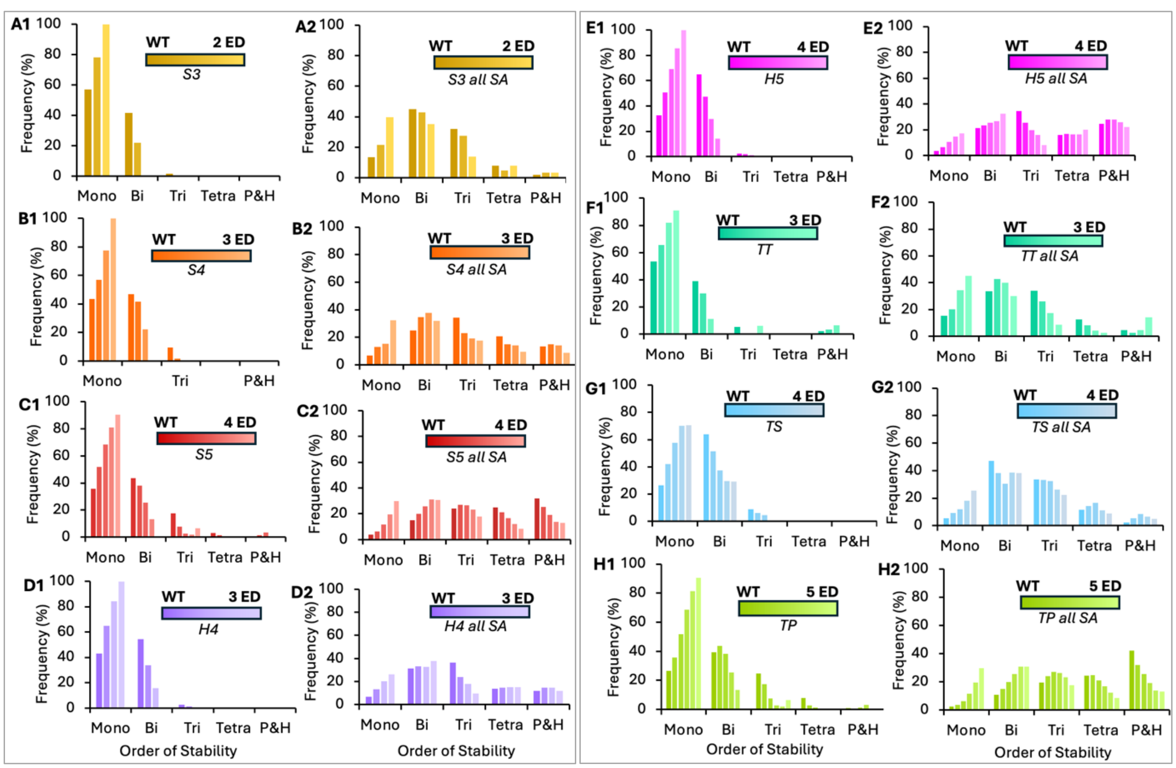

Supplementary Fig 7. Comparision of the effect of multiple edge deletions on SSD in WT and self-activated HDFLs. (A1-H1) WT HDFLs undergo multiple edge deletions that result into increase in the frequency of lower-order states, and in some cases a fully monostable network. (B1-H1) Multiple edge deletions in the same HDFLs with all nodes self-activated create almost equal chances for mono-and bistable states in small-size networks and equal possibility for mono, bi, and tristable states in relatively large networks. “WT” in A2-H2 means “WT + all nodes self-activated”.

S6. Effect of the position of edge EDs and ESRs on network dynamics.

Each of the eight networks in Fig. 7 has a self-activated (SA) terminal node and are referred to as asymmetric networks. An ED or ESR is applied at two positions in a network: P1 refers to an ED or ESR between two nodes involving a SA node. P2 refers to an ED or ESR at the other terminal of the network, i.e. the terminal that doesn’t have a SA node. The data shows that an ED at P1 can increase (decrease) more monostable (bistable) states than an ED at P2. This effect becomes more pronounced when an ED is replaced by an ESR. The data thus reveals that the position of perturbation has functional significance in networks having SA nodes (asymmetric networks). It also highlights that gene interactions that involve autoregulated genes can serve as prime targets to control multiple alternative states during fate transition.

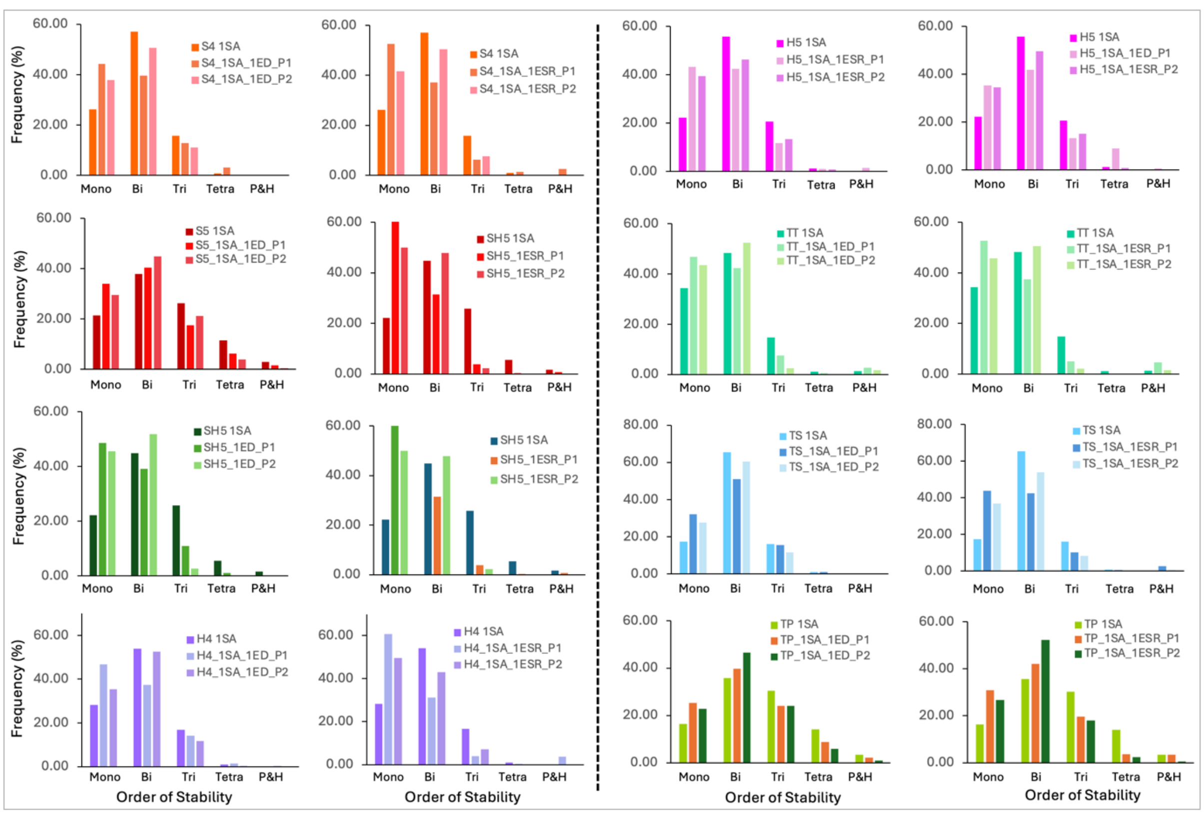

Supplementary Fig 8. Bar plots showing the effect of the position of EDs and ESRs in asymmetric networks. In each network, 1SA denotes one node is self-activated and that node is either of the terminal nodes. P1 and P2 denote the positions of ED or ESR. Each network is tested with ED and ESR at positions P1 and P2 and the SSD is compared with their unperturbed counterparts (i.e., network name_1SA). An ED or ESR at P1 reduces more bistable states and increases more monostable states than an ED or ESR at P2. Further, an ESR has a more pronounced effect than an ED. The left vertical panels show the effect of EDs at P1 and P2. The right vertical panels show the effect of ESRs at P1 and P2.

S7. Comparison of the two schemes of integration under different conditions.

In RACIPE, the default numerical integration setting has step size 0.1, initial conditions (IC) 100, maximum iterations (itr) 20, maximum production rate 10, maximum degradation rate 1, and the Euler scheme of integration. To show that our results remain invariant upon changing these parameters, we reduced step size by 10-fold, increasing the number of iterations by 5-fold, and the number of initial conditions by 10-fold (compared to default). As shown in Fig. S9, the frequencies of steady states remain unchanged. Next, we increased the production and degradation rate parameters by 10-fold each (compared to default). While this perturbation resulted in minor fluctuation in frequencies, however, it is evident that the differences are insignificant. Further, we shifted to the RK45 (Runge-Kutta order 5/4) integration scheme with a 10-fold reduction in step size and a 5-fold enhancement in the number of iterations (compared to default), we again show that the results remain unchanged. Though we present the results for S3, S4, H4, S5, and H5 networks only, the fact is that these parameter perturbations and the two different integration schemes produce the same results for all networks.

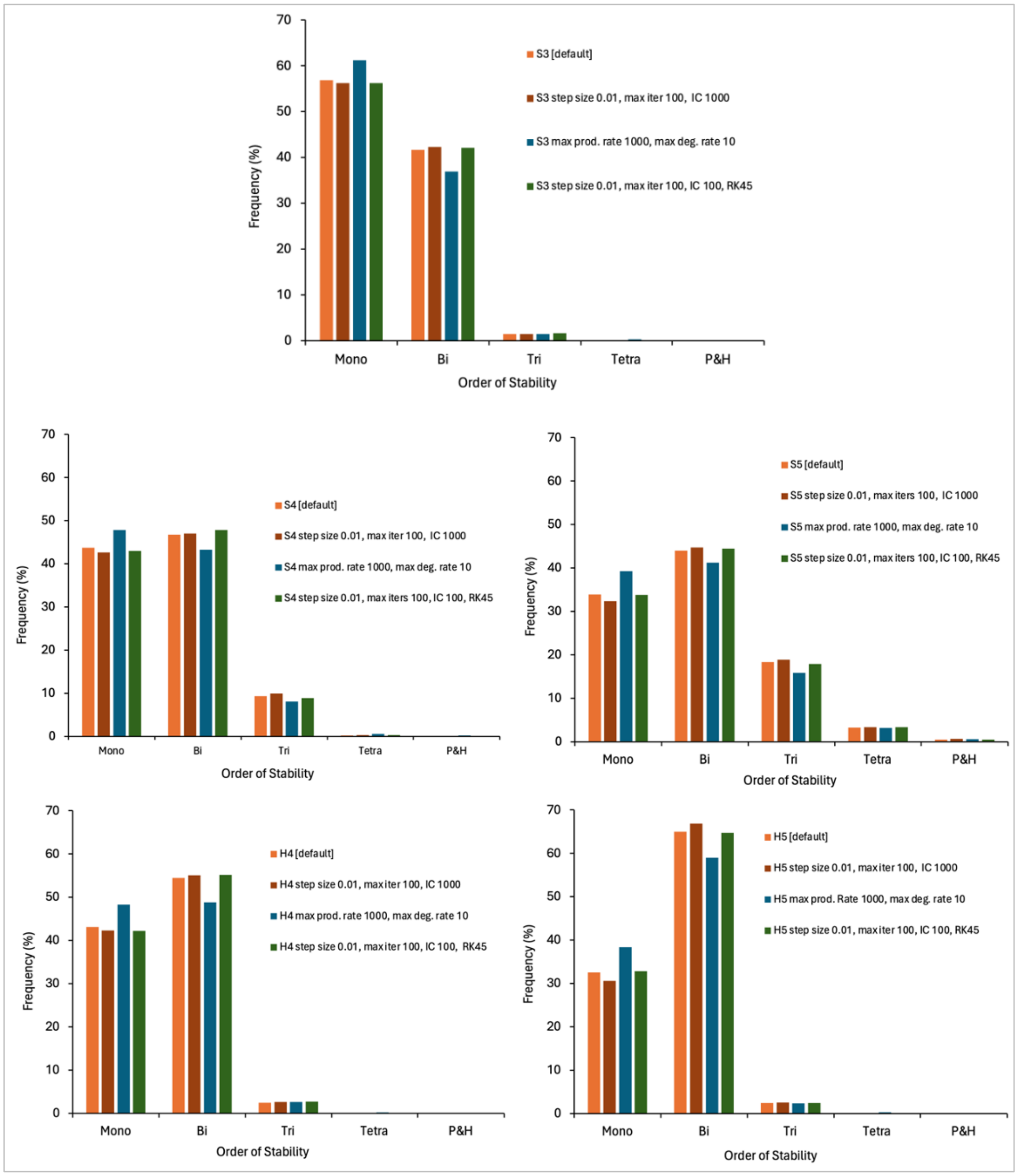

Supplementary Fig 9. Comparison of network dynamics for different parameter regimes in Euler and RK45 integration schemes.

S8. Comparison of RACIPE and Boolean simulations.

A comparison of Boolean and RACIPE simulations shows that the two approaches result in similar network dynamics as depicted by small values of JSD.

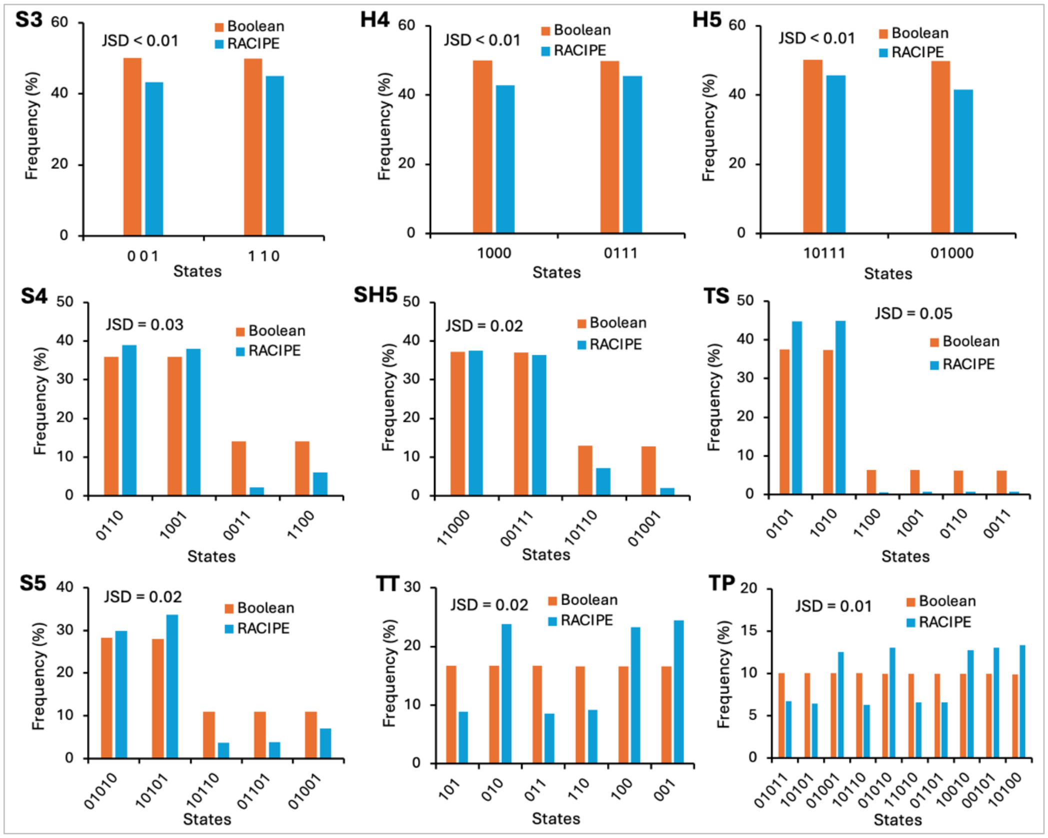

Supplementary Fig 10. Comparison of steady-state distributions of HDFLs obtained from Boolean (parameter independent) and RACIPE (parameter dependent) modeling methods. Both approaches predict a higher number of steady states in serial (S3, S4, S5) and cyclic (TT, TS, TP) networks as the number of nodes increase in these networks. On the other hand, hub networks (H4, H5) exhibit just two viable states as observed in either procedure. The Jenson-Shanon divergence (JSD) values, which range from 0 to 1, are closer to 0 for every network, implying that the frequency distributions of states predicted by Boolean and RACIPE simulations quite overlap. Technical details related to the comparison between RACIPE and Boolean simulations are elaborated in methods.

S9. Models for H5 and TP networks

Model for H5: x_1= miR200, x_2 = ZEB, x_3 = GRHL, x_4 =OVOL, x_5 = miR145

$$\dot{x_1} = B_1 + P_1\left[\left(\frac{x_{21}{}^{n_{21}}}{x_{21}{}^{n_{21}}+x_2{}^{n_{21}}}\right) + \lambda_{21}\left(\frac{x_2{}^{n_{21}}}{x_{21}{}^{n_{21}}+x_2{}^{n_{21}}}\right)\right] - d_1 * x_1$$

$$\dot{x_2} = B_2 + P_2\left[\left(\frac{x_{12}{}^{n_{12}}}{x_{12}{}^{n_{12}}+x_1{}^{n_{12}}}\right) + \lambda_{12}\left(\frac{x_1{}^{n_{12}}}{x_{12}{}^{n_{12}}+x_1{}^{n_{12}}}\right)\right]$$

$$\left[\left(\frac{x_{32}{}^{n_{32}}}{x_{32}{}^{n_{32}}+x_3{}^{n_{32}}}\right) + \lambda_{32}\left(\frac{x_3{}^{n_{32}}}{x_{32}{}^{n_{32}}+x_3{}^{n_{32}}}\right)\right]$$

$$\left[\left(\frac{x_{42}{}^{n_{42}}}{x_{42}{}^{n_{42}}+x_4{}^{n_{42}}}\right) + \lambda_{42}\left(\frac{x_4{}^{n_{42}}}{x_{42}{}^{n_{42}}+x_4{}^{n_{42}}}\right)\right]$$

$$\left[\left(\frac{x_{52}{}^{n_{52}}}{x_{52}{}^{n_{52}}+x_5{}^{n_{52}}}\right) + \lambda_{52}\left(\frac{x_5{}^{n_{52}}}{x_{52}{}^{n_{52}}+x_5{}^{n_{52}}}\right)\right] - d_2 * x_2$$

$$\dot{x_3} = B_3 + P_3\left[\left(\frac{{x_2}^{n_{23}}}{{x_{23}}^{n_{23}} + {x_2}^{n_{23}}}\right) + \lambda_{23}\left(\frac{{x_2}^{n_{23}}}{{x_{23}}^{n_{23}} + {x_2}^{n_{23}}}\right)\right] - d_3 * x_3$$

$$\dot{x_4} = B_4 + P_4\left[\left(\frac{{x_2}^{n_{24}}}{{x_{24}}^{n_{24}} + {x_2}^{n_{24}}}\right) + \lambda_{24}\left(\frac{{x_2}^{n_{24}}}{{x_{24}}^{n_{24}} + {x_2}^{n_{24}}}\right)\right] - d_4 * x_4$$

$$\dot{x_5} = B_5 + P_5\left[\left(\frac{{x_{25}}^{n_{25}}}{{x_{25}}^{n_{25}} + {x_2}^{n_{25}}}\right) + \lambda_{25}\left(\frac{{x_2}^{n_{25}}}{{x_{25}}^{n_{25}} + {x_2}^{n_{25}}}\right)\right] - d_5 * x_5$$

Model for TP: x_1= A, x_2 = B, x_3 = C, x_4 = D, x_5 = E

$$\dot{x_1} = B_1 + P_1\left[\left(\frac{{x_{21}}^{n_{21}}}{{x_{21}}^{n_{21}} + {x_2}^{n_{21}}}\right) + \lambda_{21}\left(\frac{{x_2}^{n_{21}}}{{x_{21}}^{n_{21}} + {x_2}^{n_{21}}}\right)\right]\left[\left(\frac{{x_{51}}^{n_{51}}}{{x_{51}}^{n_{51}} + {x_5}^{n_{51}}}\right) + \lambda_{51}\left(\frac{{x_5}^{n_{51}}}{{x_{51}}^{n_{51}} + {x_5}^{n_{51}}}\right)\right] - d_1 * x_1$$

$$\dot{x_2} = B_2 + P_2\left[\left(\frac{{x_{12}}^{n_{12}}}{{x_{12}}^{n_{12}} + {x_1}^{n_{12}}}\right) + \lambda_{12}\left(\frac{{x_1}^{n_{12}}}{{x_{12}}^{n_{12}} + {x_1}^{12}}\right)\right]\left[\left(\frac{{x_{32}}^{n_{32}}}{{x_{32}}^{n_{32}} + {x_3}^{n_{32}}}\right) + \lambda_{32}\left(\frac{{x_3}^{n_{32}}}{{x_{32}}^{n_{32}} + {x_3}^{n_{32}}}\right)\right] - d_2 * x_2$$

$$\dot{x_3} = B_3 + P_3\left[\left(\frac{{x_2}^{n_{23}}}{{x_{23}}^{n_{23}} + {x_2}^{n_{23}}}\right) + \lambda_{23}\left(\frac{{x_2}^{n_{23}}}{{x_{23}}^{n_{23}} + {x_2}^{n_{23}}}\right)\right]\left[\left(\frac{{x_4}^{n_{43}}}{{x_{43}}^{43} + {x_4}^{n_{43}}}\right) + \lambda_{43}\left(\frac{{x_4}^{n_{43}}}{{x_{43}}^{n_{43}} + {x_4}^{n_{43}}}\right)\right] - d_3 * x_3$$

$$\dot{x_4} = B_4 + P_4\left[\left(\frac{{x_3}^{n_{34}}}{{x_{34}}^{n_{34}} + {x_3}^{n_{34}}}\right) + \lambda_{34}\left(\frac{{x_3}^{n_{34}}}{{x_{34}}^{n_{34}} + {x_3}^{n_{34}}}\right)\right]\left[\left(\frac{{x_{54}}^{n_{54}}}{{x_{54}}^{n_{54}} + {x_5}^{n_{54}}}\right) + \lambda_{54}\left(\frac{{x_5}^{n_{54}}}{{x_{54}}^{n_{54}} + {x_5}^{n_{54}}}\right)\right] - d_4 * x_4$$

$$\dot{x_5} = B_5 + P_5\left[\left(\frac{{x_{15}}^{n_{15}}}{{x_{15}}^{n_{15}} + {x_1}^{n_{15}}}\right) + \lambda_{15}\left(\frac{{x_1}^{n_{15}}}{{x_{15}}^{n_{15}} + {x_1}^{n_{15}}}\right)\right]\left[\left(\frac{{x_{45}}^{n_{45}}}{{x_{45}}^{n_{45}} + {x_4}^{n_{45}}}\right) + \lambda_{45}\left(\frac{{x_4}^{n_{45}}}{{x_{45}}^{n_{45}} + {x_4}^{n_{45}}}\right)\right] - d_5 * x_5$$

Parameters for S3 network:

P1=20.5, x21=13.3, n21=2, λ21=0.01, d1=0.5

P2=15.7, x12=1.4, n12=2, λ12=0.01, x32=57.1, n32=1, λ32=0.01, d2=0.1

P3=14.7, x23=6.5, n23=2.0, λ23=0.03, d3=0.5

Parameters for S4 network:

P1=50.2, x21=5.5, n21=2, λ21=0.01, d1=0.6

P2=7.4, x32=1.15, n32=2, λ32=0.01, x12=55.8, n12=3, λ12=0.12, d2=0.4

P3=37.6, x43=47.6, n43=3, λ43=0.02, x23=8.5, n23=2, λ23=0.01, d3=0.3

P4=45.3, x34=13.3, n34=1, λ34=0.01, d4=0.5

Parameters for S5 network:

P1=11, x21=3.3, n21=3, λ21=0.01, d1=0.1

P2=39, x12=27.5, n12=3, λ12=0.03, x32=6.8, n32=3, λ32=0.1, d2=0.7

P3=13.2, x23=6.2, n23=4, λ23=0.07, x43=11.2, n43=2, λ43=0.08, d3=0.8

P4=28.3, x34=8.6, n34=2, λ34=0.12, x54=40.2, n54=3, λ54=0.01, d4=0.3

P5=97.310841, x45=7.550054, n45=6.000000, λ45=0.012232, d5=0.177729

Parameters for H5 network:

P1=11.5, x21=7.04, n21=2, λ21=0.01, d1=0.3

$P2=83.9$, $x12=40$, $n12=2$, $\lambda 12=0.01$, $x32=18$, $n32=1$, $\lambda 32=0.06$, $x42=24$, $n42=2$, $\lambda 42=0.01$, $x52=44.4$, $n52=2$, $\lambda 52=0.01$, $d2=0.1$

$P3=70.6$, $x23=3.6$, $n23=1$, $\lambda 23=0.02$, $d3=0.3$

$P4=81.4$, $x24=1.5$, $n24=2$, $\lambda 24=0.01$, $d4=0.9$

$P5=51.6$, $x25=8.7$, $n25=1$, $\lambda 25=0.02$, $d5=0.6$

Parameters for TP network:

$P1=60.4$, $x21=9.4$, $n21=6$, $\lambda 21=0.03$, $x51=4.9$, $n51=6$, $\lambda 51=0.01$, $d1=0.8$

$P2=63.4$, $x12=12.5$, $n12=1$, $\lambda 12=0.03$, $x32=3.4$, $n32=2$, $\lambda 32=0.01$, $d2=0.4$

$P3=80.2$, $x43=5.3$, $n43=5$, $\lambda 43=0.01$, $x23=3$, $n23=3$, $\lambda 23=0.01$, $d3=0.8$

$P4=73.5$, $x34=1.5$, $n34=5$, $\lambda 34=0.08$, $x54=12.6$, $n54=2$, $\lambda 54=0.02$, $d4=0.3$

$P5=32.7$, $x15= 4.3$, $n15=3$, $\lambda 15=0.01$, $x45=1.5$, $n45=5$, $\lambda 45=0.01$, $d5=0.8$